

# Supporting Information

## **Synthesis of Ethylenediamine Modified Tannin Polymer and Recovery of Gold(III) Ions from Electronic Wastes**

Engin Deniz Parlar<sup>1</sup>, Özge Özten<sup>2</sup>, Abdulkadir Kızılaslan<sup>3</sup>, Mustafa Can<sup>1</sup>

<sup>1</sup> Sakarya University of Applied Sciences, Faculty of Technology, Department of Metallurgical and Materials Engineering, 54050, Sakarya

<sup>2</sup> Sakarya University of Applied Sciences, Graduate Education Institute, Biomedical Engineering, 54050, Sakarya

<sup>3</sup> Sakarya University, Faculty of Engineering, Department of Metallurgical and Materials Engineering, 54050, Sakarya

<sup>4</sup> Biomedical Technologies Application and Research Center (BIYOTAM), Sakarya University of Applied Sciences, Sakarya, Turkey

## 1. Adsorption Isotherms

In order to determine which isotherm equation and its theory fitted the adsorption equilibrium state, Langmuir [1], Modified Langmuir [2], Freundlich [3], Temkin [4], Dubinin–Radushkevich [5,6] were selected to explicate precious metal ions–ATAR interactions. These isotherms and its linear forms can be seen at Table S1.

The Langmuir equation initially derived from kinetic studies has been based on the assumption that on the adsorbent surface there is a definite and energetically equivalent number of adsorption sites. The bonding to the adsorption sites can be either chemical or physical, but it must be sufficiently strong to prevent displacement of adsorbed molecules along the surface. Thus, localised adsorption was assumed as being distinct from non-localised adsorption, where the adsorbed molecules can move along the surface. Because the bulk phase is constituted by a perfect gas, lateral interactions among the adsorbate molecules were neglected. On the energetically homogeneous surface of the adsorbent a monolayer surface phase is thus formed. Langmuir, for the first time, introduced a clear concept of the monomolecular adsorption on energetically homogeneous surfaces [1,7].

The  $K_L$  and  $K_{ML}$  are the Langmuir isotherm constants. In this study, unit of  $K_L$  is L/mg and  $K_{ML}$  is dimensionless constants. Due to the Langmuir equilibrium constant,  $K_L$ , is not being dimensionless, it is not theoretically suitable for using in thermodynamic calculations. Instead, the Modified Langmuir isotherm has been proposed and the equilibrium constant is unitless [2]. The theoretical monolayer saturation capacity,  $q_m$ , dimension is given as mg/g.

**Table S1.** Adsorption isotherms and its linear forms.

	<b>Isotherm</b>	<b>Linear Form</b>	<b>X &amp; Y</b>	<b>Slope &amp; cut-off point</b>
Langmuir [1,7]	$q_e = \frac{q_m K_L C_e}{1 + K_L C_e}$	$\frac{C_e}{q_e} = \frac{1}{K_L} + \frac{\alpha_e C_e}{K_L}$	$x = C_e$ $y = C_e/q_e$	$\tan \alpha = \frac{1}{q_m}$ $cutoff = \frac{1}{K_L q_m}$
Modified Langmuir [2]	$q_e = \frac{q_m K_{ML} C_e}{(C_s - C_e) + K_{ML} C_e}$	$\frac{C_e}{q_e} = \frac{C_s}{q_m K_{ML}} + \frac{(K_{ML} - 1) C_e}{K_{ML} q_m}$		$\tan \alpha = \frac{(K_{ML} - 1)}{K_{ML} q_m}$ $cutoff = \frac{C_s}{q_m K_{ML}}$
Freundlich [3]	$q_e = K_f C_e^{1/n}$	$\log q_e = -\log K_f + \frac{1}{n} \log C_e$	$x = \log C_e$ $y = \log q_e$	$\tan \alpha = \frac{1}{n}$ $cutoff = -\log K_f$
Temkin [4]	$q_e = \frac{RT}{b} \ln (AC_e)$ , $RT/b = B$	$q_e = B \ln A + B \ln C_e$	$x = \ln C_e$ $y = q_e$	$\tan \alpha = B$ $cutoff = B \ln A$
(D-R) [5,6]	$q_e = q_m e^{-\beta \varepsilon^2}$ $\varepsilon = RT \left(1 + \frac{1}{C_e}\right)$	$\ln q_e = \ln q_m - \beta \varepsilon^2$	$x = \varepsilon^2$ $y = \ln q_e$	$\tan \alpha = \beta$ $cutoff = q_m$

The essential features of the Langmuir isotherm can be expressed in terms of a dimensionless constant called separation factor ( $R_L$ ) which is defined by the following equation

$$R_L = \frac{1}{1 + K_L C_0} \quad (1)$$

where  $C_0$  (mg/L) is the initial metal ion concentration and  $K_L$  (L/mg) is the Langmuir constant related to the energy of adsorption. In this context, the value of  $R_L$  indicates the shape of the isotherms to be either unfavorable ( $R_L > 1$ ), linear ( $R_L = 1$ ), favorable ( $0 < R_L < 1$ ) or irreversible ( $R_L = 0$ )[8,9].

The Freundlich isotherm is an empirical equation employed to describe heterogeneous systems and equation shown in Table S2. In this equation,  $K_f$ , ( $mg^{1-1/n} L^{1/n} g^{-1}$ ) is the Freundlich constant related to the bonding energy, and  $n$ , ( $g/L$ )

is the heterogeneity factor. The slope  $(1/n)$  ranges between 0 and 1 is a measure of adsorption intensity or surface heterogeneity, and it becomes more heterogeneous when its value gets closer to zero. Whereas, a value below unity implies chemisorption process where  $1/n$  above one is an indicative of cooperative adsorption [8,10].

By ignoring the extremely low and large value of concentrations, the derivation of the Temkin isotherm assumes that the fall in the heat of sorption is linear rather than logarithmic. Temkin equation is excellent for predicting the gas phase equilibrium, conversely complex adsorption systems including the liquid-phase adsorption isotherms are usually not appropriate to be represented [11]. In this equation,  $A$  (L/mg) is the equilibrium binding constant corresponding to the maximum binding energy,  $b$  (J/mol) is Temkin isotherm constant and constant  $B$  (dimensionless) is related to the heat of adsorption.

Radushkevich [5] and Dubinin [12] have reported that the characteristic sorption curve is related to the porous structure of the sorbent (Table S1). Where the constant,  $\beta$ , ( $\text{mmol}^2/\text{J}^2$ ) is D-R constant related to the mean free energy of sorption per mole of the sorbate as it is transferred to the surface of the solid from infinite distance in the solution and can be correlated using following relationship

$$E = \frac{1}{\sqrt{2\beta}} \quad (2)$$

and  $q_m$ , (mmol/g) is denoted as the single layer capacity. In a deeper explanation,  $E$  value indicates the mechanism of the adsorption reaction. When  $E < 8 \text{ kJ/mol}$ , physical forces may affect the adsorption. If  $E$  is  $8 < E < 16 \text{ kJ/mol}$ , adsorption is governed by ion exchange mechanism, while for the values of  $E > 18 \text{ kJ/mol}$ , adsorption may be

dominated by particle diffusion [13]. The model has often successfully fitted high solute activities and the intermediate range of concentrations data well, but has unsatisfactory asymptotic properties and does not predict the Henry's law at low pressure [8,13]. Meanwhile, the parameter  $\varepsilon$  known as Polanyi potential and can be correlated as

$$\varepsilon = RT \left( 1 + \frac{1}{C_e} \right) \tag{3}$$

where  $R$ ,  $T$  and  $C_e$  represent the gas constant (8.314 J/mol K), absolute temperature (K) and adsorbate equilibrium concentration (mg/L), respectively.

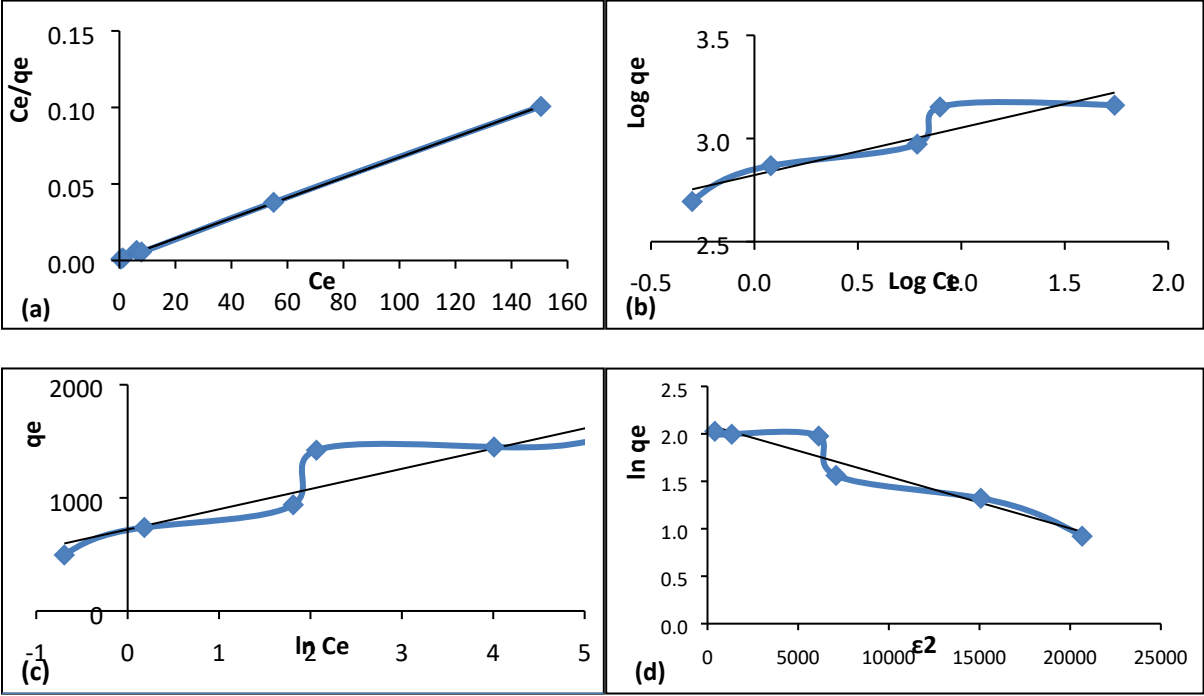


**Figure S1.** (a) Langmuir and Modified Langmuir isotherm at 328 K temperature for Au(III) - ATAR polymer adsorption system, (b) Freundlich, (c) Temkin (d), Dubinin – Raduskevich isotherm

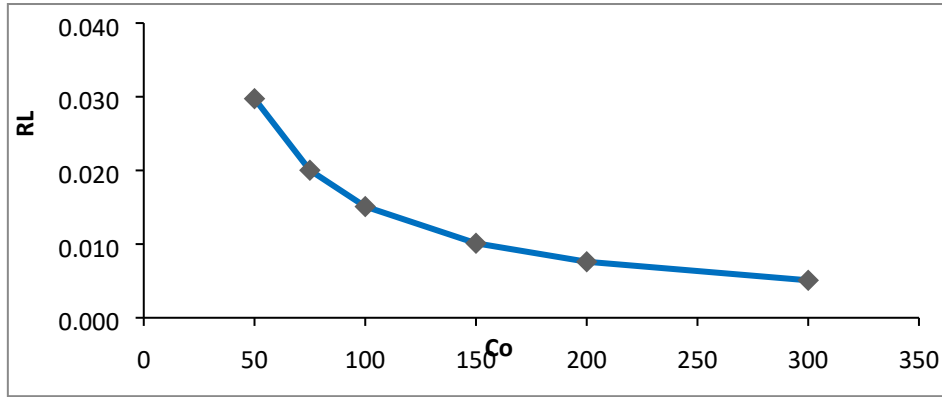


**Figure S2.**  $R_L$  changes at 328 K for the Au(III)-ATAR polymer adsorption system

The experimental data required for the isotherm calculations in the Au(III) - ATAR polymer adsorption system are given in Table S2 – S4 for the temperature values of 298 K, 308 K, 318 K.

**Table S2.** Experimental isotherm data at 298 K temperature for Au(III)-ATAR adsorption system.

$C_0$ (mg/L)	50	75	100	150	200	300
$C_e$ (mg/L)	1,2	2,0	11,2	36,5	85,0	184,4
$q_e$ (mg/g)	487,6	730,0	888,0	1135,0	1150,0	1156,2

**Table S3.** Experimental isotherm data at 308 K temperature for Au(III)-ATAR adsorption system.

$C_0$ (mg/L)	50	75	100	150	200	300
$C_e$ (mg/L)	1,0	1,9	10,2	29,6	79,1	175,7
$q_e$ (mg/g)	489,9	731,5	897,6	1204,5	1208,8	1243,5

**Table S4.** Experimental isotherm data at 318 K temperature for Au(III)-ATAR adsorption system.

$C_0$ (mg/L)	50	75	100	150	200	300
$C_e$ (mg/L)	0,9	1,8	9,3	27,0	76,2	170,5
$q_e$ (mg/g)	491,0	732,200	907,5	1230,1	1237,6	1294,9

In Table S5-S7, isotherm constants at 298 K, 308 K, 318 K temperatures are given for the Au(III)-ATAR adsorption system.

**Table S5.** Isotherm constants at 298 K temperature for the Au(III)-ATAR adsorption system.

Isotherm	$K_L$ and $K_{LM}$	$Q_{max}$ (mg/g)	$R_L$	$R^2$	$x^2$	$a_L$ (L/mg)	S.S.
Langmuir	579.98 L/mg	1178.59	0.0134	0.9992	46.289	0.4921	0.125
Modifiye Langmuir	216607.1	1178.59		0.9992	46.289		0.125
Freundlich	$K_f$ (L/g)	$n$		$R^2$	$x^2$		S.S.
	0.018	5.44		0.8795	46.289		0.125
Temkin	A (L/g)	B (j/mol)		$R^2$	$x^2$		S.S.

	37.349	149.014		0.9334	30.373	0.110
<b>Dubinin - Radoskevich</b>	$\beta$ (mmol/J) <sup>2</sup>	$q_m$ (mmol /g)	$E$ (kJ/mol)	$R^2$	$x^2$	<b>S.S.</b>
	0.0001	6.2282	95.6199	0.9245	24.655	0.095

**Table S6.** Isotherm constants at 308 K temperature for the Au(III)-ATAR adsorption system.

<b>Isotherm</b>	$K_L$ and $K_{LM}$	$Q_{max}$ (mg/g)	$R_L$	$R^2$	$x^2$	$a_L$ (L/mg)	<b>S.S.</b>
<b>Langmuir</b>	635.10 L/mg	1241.11	0.0129	0.9986	56.22	0.5117	0.138
<b>Modifiye Langmuir</b>	225239.1	1241.11		0.9986	56.22		0.138
<b>Freundlich</b>	$K_f$ (L/g)	$n$		$R^2$	$x^2$		<b>S.S.</b>
	0.018	5.1		0.8992	45.85		0.121
<b>Temkin</b>	$A$ (L/g)	$B$ (j/mol)		$R^2$	$x^2$		<b>S.S.</b>
	29.8061	163.724		0.9362	29.33		0.1003
<b>Dubinin - Radoskevich</b>	$\beta$ (mmol/J) <sup>2</sup>	$q_m$ (mmol /g)	$E$ (kJ/mol)	$R^2$	$x^2$		<b>S.S.</b>
	0.0001	6.6015	94.85	0.9425	24.54		0.089

**Table S7.** Isotherm constants at 318 K temperature for the Au(III)-ATAR adsorption system.

<b>Isotherm</b>	$K_L$ and $K_{LM}$	$Q_{max}$ (mg/g)	$R_L$	$R^2$	$x^2$	$a_L$ (L/mg)	<b>S.S.</b>
<b>Langmuir</b>	681.38 L/mg	1270.206	0.0123	0.9987	55.39	0.5364	0.138
<b>Modifiye Langmuir</b>	236090.9	1270.206		0.9987	55.39		0.138
<b>Freundlich</b>	$K_f$ (L/g)	$n$		$R^2$	$x^2$		<b>S.S.</b>
	0.017	4.9851		0.9085	46.37		0.118
<b>Temkin</b>	$A$ (L/g)	$B$ (j/mol)		$R^2$	$x^2$		<b>S.S.</b>
	28.5864	169,746		0.9418	26.93		0.093
<b>Dubinin - Radoskevich</b>	$\beta$ (mmol/J) <sup>2</sup>	$q_m$ (mmol /g)	$E$ (kJ/mol)	$R^2$	$x^2$		<b>S.S.</b>
	0.0001	6.7944	94.7937	0.9544	21.63		0.081

## 2. Adsorption Kinetics

Adsorption kinetics that is examining the change of adsorption on solid surfaces from solutions up to reaching equilibrium, a suitable kinetic model is needed to analyze the rate data. With the development of the adsorption equilibrium theory on heterogeneous solid surfaces, the development of the kinetic adsorption-desorption theory has also progressed [10]. In order to understand best fitting the kinetic theory and its equation of studied metal ion adsorption kinetics, the pseudo first and pseudo second order, Elovich, and intraparticle diffusion equations were applied. These isotherms, linear forms, and their constants can be seen at **Table S8**.

**Table S8.** Used adsorption kinetic equations and its linear forms.

<b>Equation</b>	<b>Linear Form</b>	<b>Constants</b>
-----------------	--------------------	------------------

<b>Lagergren first-order</b> [14]	$\frac{dq_t}{dt} = k_1(q_e - q_t)$	$\log(q_e - q_t) = \log q_e - \frac{k_1}{2,303}t$	$k_1 (\text{min.}^{-1})$
<b>Pseudo second-order</b> [15]	$\frac{dq_t}{dt} = k_2(q_e - q_t)^2$	$\frac{t}{q_t} = \frac{1}{kq_e^2} + \frac{1}{q_e}t$	$k_2(\text{g.mg}^{-1}.\text{min.}^{-1})$
<b>Elovich</b> [16,17]	$\frac{dq_t}{dt} = \alpha e^{-\beta q_t}$	$q_t = \frac{1}{\beta} \ln(\alpha \beta) + \frac{1}{\beta} \ln t$	$\alpha (\text{mg.g}^{-1}.\text{min.}^{-1})$ $\beta (\text{mg.g}^{-1})$
<b>Intraparticle diffusion</b> [5]	$q_t = k_{int}t^{1/2}$		$k_{int} (\text{mg.g}^{-1}.\text{min.}^{-\frac{1}{2}})$

An adsorption-desorption kinetics can include the following four steps: external diffusion from solution to interface, diffusion into pores, diffusion of molecules on surface, and realization of adsorption-desorption process [7,10]. Integrated linear pseudo-first and pseudo-second order, Elovich, and intraparticle diffusion kinetic equation form function graphics and their R<sup>2</sup> values can be seen in **Figure S3**.

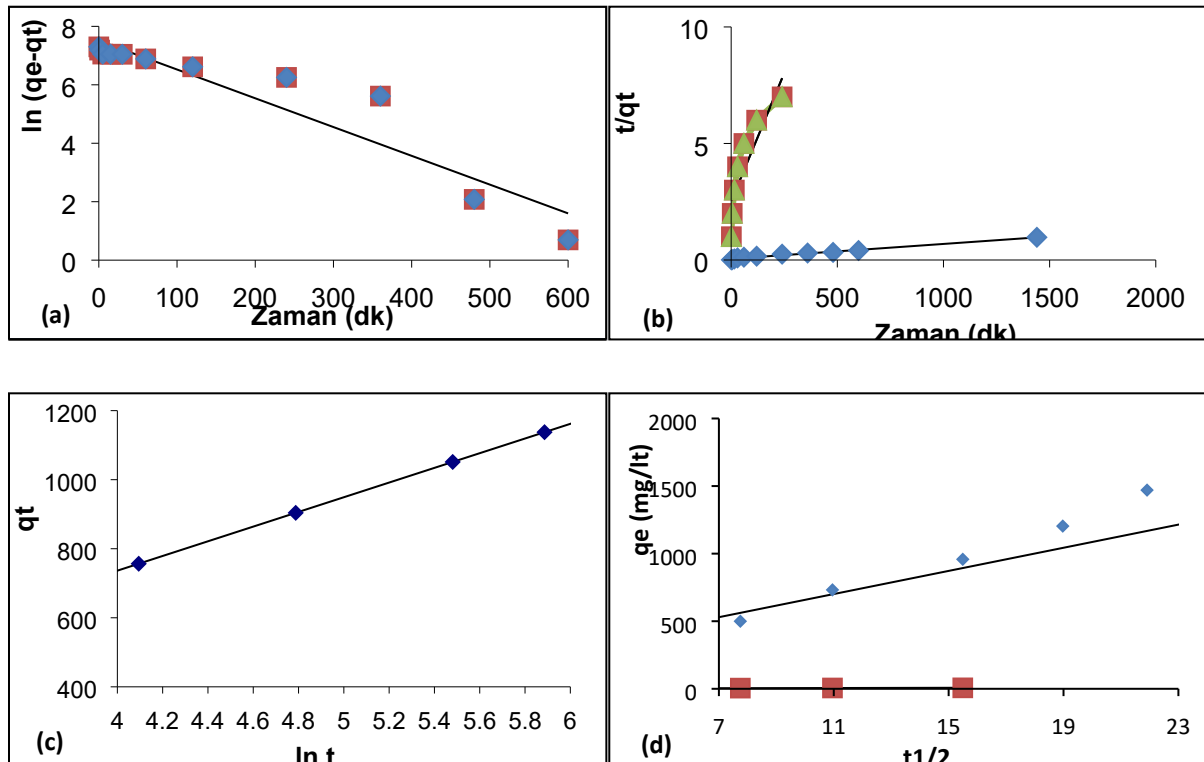


**Figure S3.** Comparison of the agreement of (a) pseudo first order, (b) pseudo second order, (c) Elovich, and (d) intraparticle diffusion kinetic equations with experimental data (temperature = 298 K, volume = 500 mL, C<sub>0</sub> = 150 mg/L, pH (temperature = 298 K, volume = 500) mL, C<sub>0</sub> = 150 mg/L, pH = 2, adsorbent mass = 50 mg)

### 3. Adsorption Thermodynamic



Thermodynamic parameters such as Gibb's free energy ( $\Delta G^0$ ), enthalpy change ( $\Delta H^0$ ) and change in entropy ( $\Delta S^0$ ) for the adsorption of metal ions on ATAR have been determined by using the following equations

$$\Delta G^0 = \Delta H^0 - T\Delta S^0 \quad (6)$$

$$\Delta G^0 = -RT \ln(K_{ML}) \quad (7)$$

$$\log(K_{ML}) = \frac{\Delta S^0}{2.303 R} - \frac{\Delta H^0}{2.303 RT} \quad (8)$$

where  $q_e$  is the amount of metal ion adsorbed per unit mass of beads (mg/g),  $C_e$  is equilibrium concentration (mg/L) and  $T$  is temperature in K and  $R$  is the gas constant (8.314 J/molK).  $K_{LM}$  is dimensionless Modified Langmuir constant at each temperature. It is calculated from linear regression solve of isotherm equation. Considering the relationship between  $\Delta G^0$  and  $K_L$ ,  $\Delta H^0$  and  $\Delta S^0$  were determined from the slope and intercept of the van't Hoff plots of  $\log(K_{ML})$  versus  $1/T$ . This pilot can be seen at Figure S4 at the manuscript. Negative values of  $\Delta G^0$  confirm the feasibility of the process and the spontaneous nature of the adsorption [13]. The positive value of  $\Delta H^0$  is indicating that the adsorption reaction was endothermic. The negative entropy change ( $\Delta S^0$ ) for the process was caused by the decrease in degree of freedom of the adsorbed species [11].

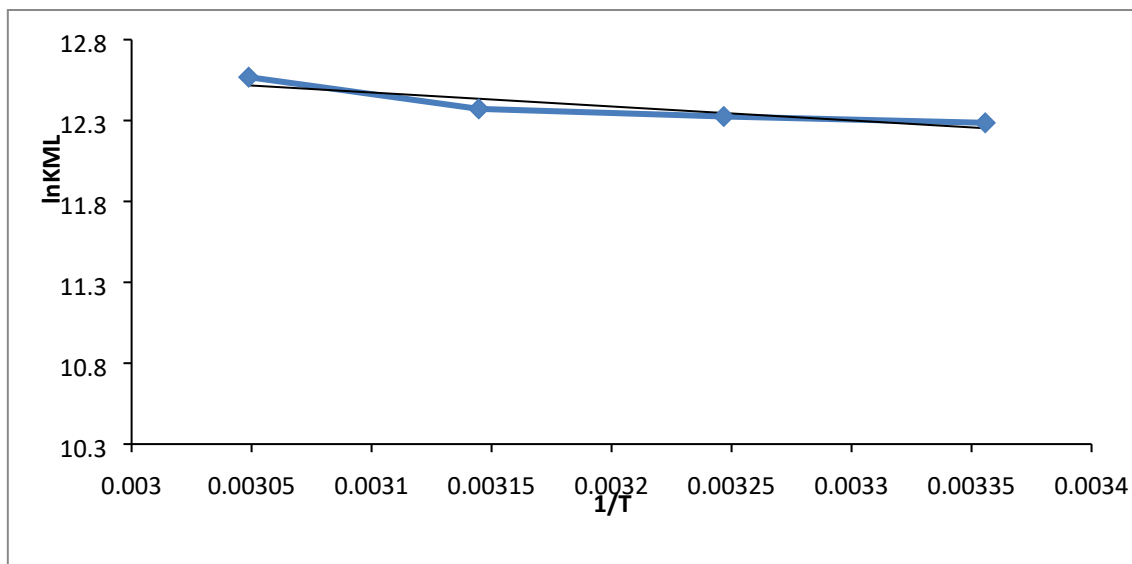


**Figure S4.**  $\log K_{ML} - 1/T$  değerleri  $\log K_{ML} - 1/T$  values in Au(III) ion adsorption onto ATAR particles.

#### 4. Recovery of Precious Metals from e-wastes

In Table S9, the adsorption capacity ( $q_e$ ) values of the ATAR polymer in hydrochloric acid leaching solution for each metal ion examined are shown.

**Table S9.** The amount of metal adsorbed on the adsorbent surface after adsorption (1 hour, 10 mL, pH = 2, 328 K)

Adsorbent mass	Adsorption capacity, $q_e$ , (mg/g)											
	Al	Fe	Ni	Cu	Zn	Pd	Ag	Sn	Sb	Pt	Au	Pb
10 mg	0.29	0.34	5.51	151.25	0.02	0.28	22.4	385.4	22.3	0.03	776.78	27.69
30 mg	3.43	1.20	9.79	241.04	0.34	0.41	23.7	513.7	24.0	0.04	776.84	30.36
50 mg	4.78	1.39	11.4	242.12	0.62	0.42	25.3	516.8	24.2	0.04	777.08	30.45
100 mg	4.91	2.47	16.6	308.84	0.93	0.46	25.8	606.2	25.8	0.05	777.19	30.89
200 mg	5.57	3.30	18.0	337.33	1.06	0.47	26.2	611.5	26.0	0.05	777.19	32.51

## REFERENCES

- [1] I. Langmuir, The adsorption of gases on plane surfaces of glass, mica and platinum, J. Am. Chem. Soc. 40 (1918) 1361–1403.
- [2] S. Azizian, S. Eris, L.D. Wilson, Re-evaluation of the century-old Langmuir isotherm for modeling adsorption phenomena in solution, Chem. Phys. 513 (2018) 99–104. <https://doi.org/10.1016/j.chemphys.2018.06.022>.
- [3] H. Freundlich, Über die adsorption in lösungen, Zeitschrift Für Phys. Chemie. 57 (1907) 385–470.
- [4] M.I. Temkin, Kinetics of ammonia synthesis on promoted iron catalysts., Acta Physiochim. URSS. 12 (1940) 327–356.
- [5] M.M. Dubinin, The potential theory of adsorption of gases and vapors for adsorbents with energetically nonuniform surfaces, Chem. Rev. 60 (1960) 235–241.

- [6] M.M. Dubinin, Fundamentals of the theory of adsorption in micropores of carbon adsorbents: Characteristics of their adsorption properties and microporous structures, *Carbon* N. Y. 27 (1989) 457–467.
- [7] Y. Liu, Y.J. Liu, Biosorption isotherms, kinetics and thermodynamics, *Sep. Purif. Technol.* 61 (2008) 229–242. <https://doi.org/10.1016/j.seppur.2007.10.002>.
- [8] K.Y. Foo, B.H. Hameed, Insights into the modeling of adsorption isotherm systems, *Chem. Eng. J.* 156 (2010) 2–10. <https://doi.org/10.1016/j.cej.2009.09.013>.
- [9] T.W. Weber, R.K. Chakravorti, Pore and solid diffusion models for fixed-bed adsorbers, *AIChE J.* 20 (1974) 228–238. <https://doi.org/10.1002/aic.690200204>.
- [10] A. Dąbrowski, Adsorption - From theory to practice, *Adv. Colloid Interface Sci.* 93 (2001) 135–224. [https://doi.org/10.1016/S0001-8686\(00\)00082-8](https://doi.org/10.1016/S0001-8686(00)00082-8).
- [11] M. Can, Equilibrium, kinetics and process design of acid yellow 132 adsorption onto red pine sawdust, *Water Sci. Technol.* 71 (2015) 1901–1911. <https://doi.org/10.2166/wst.2015.164>.
- [12] M.M. Dubinin, Adsorption in micropores, *J. Colloid Interface Sci.* 23 (1967) 487–499. [https://doi.org/10.1016/0021-9797\(67\)90195-6](https://doi.org/10.1016/0021-9797(67)90195-6).
- [13] M. Can, Investigation of the factors affecting acid blue 256 adsorption from aqueous solutions onto red pine sawdust: equilibrium, kinetics, process design, and spectroscopic analysis, *Desalin. Water Treat.* 57 (2016) 5636–5653. <https://doi.org/10.1080/19443994.2014.1003974>.
- [14] S. Lagergren, About the theory of so-called adsorption of soluble substances (org.: Zur theorie der sogenannten adsorption gelöster stoffe), *K. Sven. Vetenskapsakademiens Handl.* 24 (1898) 1–39.
- [15] G. Ho, Y. S., McKay, Pseudo-second order model for sorption processes, *Process Biochem.* 34 (1999) 451–465.
- [16] Ya. B. Zeldovich, Theoretical foundations of combustion processes, *Acta Physicochim. U.R.S.S.* 1 (1934) 449–469.
- [17] G.M. Elovich, S. Y., & Zhabrova, Mechanism of the catalytic hydrogenation of ethylene on nickel. I. Kinetics of the process., *J. Phys. Chem.* 13 (1939) 1761.